*Plant Physiology*, January 1999, Vol. 119, pp. 111–121, www.plantphysiol.org © 1999 American Society of Plant Physiologists

# Dynamics of Cytokinins in Apical Shoot Meristems of a Day-Neutral Tobacco during Floral Transition and Flower Formation[1]

**Walter Dewitte, Adriana Chiappetta, Abdelkrim Azmi, Erwin Witters, Miroslav Strnad, Jacques Rembur, Michelle Noin, Dominique Chriqui, and Henri Van Onckelen***

Laboratory for Plant Biochemistry and Physiology, Department of Biology, University of Antwerp, B-2610 Antwerp, Belgium (W.D., E.W., H.V.O.); Laboratory Cytologie Expérimentale et Morphogenèse Végétale, Pierre and Marie Curie University, F-75252 Paris cedex 05, France (A.C., A.A., J.R., M.N., D.C.); Laboratory of Growth Regulators, Department of Botany, Palacky´ University and Institute of Experimental Botany, Academy of Sciences of the Czech Republic, 78371 Olomouc, Czech Republic (M.S.)

**This study considered cytokinin distribution in tobacco (*Nicotiana tabacum* L.) shoot apices in distinct phases of development using immunocytochemistry and quantitative tandem mass spectrometry. In contrast to vegetative apices and flower buds, we detected no free cytokinin bases (zeatin, dihydrozeatin, or isopentenyladenine) in prefloral transition apices. We also observed a 3-fold decrease in the content of cytokinin ribosides (zeatin riboside, dihydrozeatin riboside, and isopentenyladenosine) during this transition phase. The group concluded that organ formation (e.g. leaves and flowers) is characterized by enhanced cytokinin content, in contrast to the very low endogenous cytokinin levels found in prefloral transition apices, which showed no organogenesis. The immunocytochemical analyses revealed a differing intracellular localization of the cytokinin bases. Dihydrozeatin and isopentenyladenine were mainly cytoplasmic and perinuclear, whereas zeatin showed a clear-cut nuclear labeling. To our knowledge, this is the first time that this phenomenon has been reported. Cytokinins do not seem to act as positive effectors in the prefloral transition phase in tobacco shoot apices. Furthermore, the differences in distribution at the cellular level may be indicative of a specific physiological role of zeatin in nuclear processes.**

Cytokinins have been arbitrarily defined as factors capable of promoting growth of cultured plant cells (Skoog and Miller, 1957). Chemically, known natural cytokinins are the $N^6$-substituted adenines and their riboside, ribotide, and glycoside conjugates. The diversity of the $N^6$ substituents is the origin of the different cytokinin types. Aside from the well-documented stimulatory effect of added cytokinins on growth and differentiation of cultured plant cells, flowering is among the many other developmental processes that cytokinins have been reported to mediate in plants (Mok, 1994). Altered cytokinin concentrations before and after flower induction have been reported for some species (Lejeune et al., 1988, 1994; de Bouillé et al., 1989). Intervention in the signal-transduction cascade caused by decreasing the cytokinin sensitivity in Arabidopsis resulted in a pleiotropic effect that included the formation of a single, infertile flower (Deikman and Ulrich, 1995). This effect was more complex than a dose response; it was demonstrated in Arabidopsis that the effect of an aromatic cytokinin on the flowering program was dependent on the developmental stage of the apical shoot meristem (Besnard-Wibaut, 1981; Venglat and Sawhney, 1996).

Research on the involvement of cytokinins in flowering and other physiological phenomena requires accurate techniques to study the distribution and concentration on a cellular and tissue level. To meet these demands, research groups have adopted two strategies. One consists of improving the detection limit and specificity of the analytical chemistry techniques used for quantification of endogenous hormone levels (Prinsen et al., 1995). The other focuses on the elaboration of techniques for in situ localization of hormones (Zavala et al., 1983; Eberle et al., 1987; Sotta et al., 1990; Ivanova et al., 1994).

We report changes in the endogenous cytokinin content in the shoot apex of tobacco (*Nicotiana tabacum* L.) during distinct phases of the transition from a vegetative to a reproductive status. We obtained the data by combining an accurate procedure for immunolocalization of three different cytokinin bases, zeatin, DHZ, and IP, and capillary liquid chromatography-tandem MS (E. Witters, K. Vanhoutte, W. Dewitte, I. Machackova, E. Benkova, W. Van Dongen, E. Esmans, and H.A. Van Onckelen, unpublished data), a highly sensitive technique for the quantification of cytokinins. The immunocytochemical study focused on cytokinin bases that were postulated to be the main active

[1] W.D. was a recipient of an Individual Human Capital and Mobility Fellowship (no. ERBCHBICT941211). H.V.O. is a Research Director at the Flemish Fund for Scientific Research, Belgium. This research was also supported by a grant from the Belgian Program on Interuniversity Poles of Attraction (Prime Minister's Office, Science Programming, no. 15) and by the granting agency of the Czech Republic (no. 206 196/K 188).

* Corresponding author; e-mail hvo@uia.ua.ac.be; fax 1–32–3–820–22–71.

Abbreviations: AP, alkaline phosphatase; DHZ, dihydrozeatin; DHZR, dihydrozeatin riboside; FITC, fluorescein-5-isothiocyanate; IP, isopentenyladenine; IPA, isopentenyladenosine; ZR, zeatin riboside.

forms (Laloue and Pethe, 1982). At the molecular level the potential of naturally occurring $N^9$-substituted cytokinins to inhibit starfish $p34^{cdc2}$/cyclin B kinase activity by competing with ATP in vitro was less than the inhibiting potential of the free bases (Veselý et al., 1994); however, it remains difficult to explain cytokinin action solely by means of this competition model, because stimulation of a tobacco $p34^{cdc2}$-like kinase in vivo by cytokinins was also reported (Zhang et al., 1996).

Based on the observed dynamics of endogenous levels and in situ localization of different cytokinins at the cellular and tissue level, our study discusses their putative roles in developmental processes such as leaf initiation, floral induction, and flower formation.

## MATERIALS AND METHODS

### Plant Material

Tobacco (*Nicotiana tabacum* L. var. Petit Havana SR1) seeds were germinated in compost (Sterlux, Barbin S.A., Rungis, France) in open, plastic containers in the greenhouse with day and night temperatures of about 25°C and 20°C, respectively. A 16-h photoperiod was obtained with fluorescent tubes (Truelight, Grolux, Sylvania, and Mazdafluor, Mazda-Philips, Paris, France) dispensing 90 $\mu$mol $m^{-2}$ $s^{-1}$. After 2 weeks the plantlets were transferred to small, individual pots. At the three-leaf stage they were transferred to larger pots until harvesting. Shoot apices for immunolocalization and extraction were collected during the vegetative, transitional, and reproductive phases (Fig. 1).

### Chemicals

Unless stated otherwise, Merck (Overijse, Belgium) provided the chemicals.

### Immunological Reagents

Coupling of cytokinin ribosides (ZR, DHZ, and IPA) (Apex International, Honiton, UK) to BSA was achieved by the periodate oxidation method (Erlanger and Beiser, 1964). We calculated a coupling ratio of 3 to 9 mol of the appropriate cytokinin per mol BSA from the UV spectra of the conjugates. The antigens were dissolved in PBS (25 mM $Na_2HPO_4$ and 0.15 M NaCl, pH 7.4) at 0.5 mg $mL^{-1}$ and mixed with an equal volume of Freund's complete adjuvant. New Zealand White rabbits were immunized by multiple-site subcutaneous injections of 200 $\mu$g of conjugates given at d 0, 7, 28, 42, 72, and 132. We bled the animals 7 d after the last injection and stored the sera at −20°C.

### Preparation of Cytokinin-Affinity Columns

Cytokinin ribosides (50 $\mu$mol) were dissolved in 500 $\mu$L of dimethylformamide, and 100 $\mu$mol of solid $NaIO_4$ was added. The mixture was stirred in the dark for 15 min. Adding 90 $\mu$mol of ethylene glycol stopped the reaction. After 5 min the reaction mixture was applied dropwise to 5 mL of poly-L-Lys agarose (Sigma) slurried in 1 mL of borate buffer (25 mM $Na_2B_4O_7$ and 15 mM NaCl, pH 9.5) and stirred for 60 min in the dark. The coupling reaction was stabilized overnight at 4°C with an excess of $NaBH_3CN$ (250 $\mu$mol). The cytokinin affinity sorbent (5 mL) was packed into a 10-mL polypropylene syringe and washed consecutively with 5 volumes of PBS, 2 M NaCl in PBS, PBS, water, methanol, water, 0.1 M glycine-HCl (pH 2.5, saturated with diethyl ether), water, and PBS containing 0.1% (w/v) $NaN_3$. We determined a theoretical column capacity of 7 to 15 mg IgG $mL^{-1}$ of poly-L-Lys agarose from the difference in the UV spectra of the sorbents.

### Purification of Cytokinin Antibodies by Affinity Chromatography

Two milliliters of rabbit serum diluted five times in PBS (pH 7.5, 37°C) was allowed to flow through the affinity column for at least 1 h. The columns were subsequently washed with 5 volumes of PBS, pH 7.5, and 2 M NaCl in PBS. Columns were eluted with Gly-HCl (pH 2.5, 4°C, saturated with diethyl ether) until the $A_{280}$ was enhanced (SP8440 XR, Spectra Physics, San Jose, CA). UV-absorbing fractions (1 mL) were collected into 350 $\mu$L of ice-cold 1 M Tris-HCl, pH 8.0. Fractions were combined and the ether was rapidly removed by rotary evaporation at 25°C. Purified antibodies were precipitated with 100% (v/v) of saturated ammonium sulfate solution (1 h at 4°C), followed by centrifugation at 3000*g* (4°C). We discarded the supernatant and dissolved the pellet in 1 mL of PBS. The antibody solution was dialyzed against five 2-L changes of PBS (supplemented with 0.04% [w/v] $NaN_3$) at 4°C; we determined the protein content by measuring the $A_{280}$ (UV-2101PC, Shimadzu, Kyoto, Japan). Glycerin was added until a 50% (v/v) final concentration was reached. This stock solution was divided into aliquots of 100 $\mu$L and stored at −20°C until use. After affinity purification and dialysis all affinity-purified sera had a protein content between 0.8 and 1.5 mg $mL^{-1}$.

### Determination of the Cross-Reactivity of the Sera

We used ELISA to screen for cross-reactivity of the sera to different compounds (Strnad et al., 1992) and coated the wells of an ELISA plate (Maxisorb, Nunc, Roskilde, Denmark) with 150 $\mu$L of 5 $\mu$g $mL^{-1}$ antibody solution in PBS, pH 7.2, at 4°C overnight. After saturating remaining binding sites with 0.5% (w/v) BSA in PBS for 1 h, we pipetted 50 $\mu$L of PBS, 50 $\mu$L of cytokinin riboside linked to AP (Boehringer Mannheim), and 50 $\mu$L of the different diluted compounds into the wells. After 1 h of incubation and several consecutive washes with 3× PBS, water, and Tris buffer (pH 9.6, 2 mM $MgCl_2$), we added 4-nitrophenyl disodium phosphate (1 mg $mL^{-1}$ in Tris-HCl buffer, 0.1 M, pH 9.6, and 2 mM $MgCl_2$), and incubated the plate for 1 h at 37°C. We measured competition by monitoring the $A_{405}$ (EAR 400, SLT, Grödig, Austria).

### Fixation Efficiency Testing

To determine the fixation of the cytokinin bases in vitro, we coated the wells of an ELISA plate overnight with 150 $\mu$L of 0.5% (w/v) BSA solution, rinsed them with distilled water, and treated them with 20 nmol of zeatin, DHZ, IP, or their ribosides dissolved in a 3% (w/v) paraformaldehyde and a 0.5% (v/v) glutaraldehyde (LADD Research Industries, Williston, VT) mixture in PBS. After 3 h at 4°C, wells were washed with distilled water, and 150 $\mu$L of PBS buffered primary antibody solution in the same dilution as used for immunolabeling was pipetted into the wells and incubated overnight at 4°C. After rinsing with PBS, we used AP-conjugated sheep anti-rabbit immunoglobulins (1:100) (Boehringer Mannhein) as secondary antibodies. 4-Nitrophenyl phosphate disodium salt (1 mg $mL^{-1}$) was provided as a substrate for the AP, and the reaction product was monitored at $A_{405}$ after 15 min at room temperature.

The binding of cytokinin bases and ribosides to plant tissues was determined by means of radioactive cytokinins: 1.7 kBq of tritium-labeled cytokinin base or riboside (*trans*[2-$^3$H]zeatin, 0.9 TBq $mmol^{-1}$; [$^3$H]DHZ, 1.27 TBq $mmol^{-1}$; [2-$^3$H]IP, 1.65 TBq $mmol^{-1}$; [2-$^3$H]ZR, 0.9 TBq $mmol^{-1}$; [$^3$H]DHZ, 1.27 TBq $mmol^{-1}$; and [2-$^3$H]IPA, 1.65 TBq $mmol^{-1}$; Institute of Experimental Botany, Prague, Czech Republic) was added to 200 $\mu$L of fixative (3% [w/v] paraformaldehyde and 0.5% [v/v] glutaraldehyde in PBS, pH 7.2). The fixative, supplemented with the radioactive tracers, was allowed to react with fresh tobacco stem sections approximately 1 mm thick for 3 h at 4°C. The tissue was washed in PBS (5 × 10 min) and dissolved in 3 mL of Soluene 350 (Packard Instruments, Groningen, The Netherlands) before liquid-scintillation counting (Tri Carb 1500, Packard Instruments). The results were expressed as a percentage of the total radioactivity added, and the fresh weight of the stem sections was used for normalization of the radioactivity measured in the tissue.

### Mitotic Index Determination

Mitotic activity was quantified on longitudinal sections of shoot apices excised at various developmental stages. The apices were fixed by ethanol:acetic acid (3:1, v/v), and then stained according to the Feulgen reaction (1 N HCl hydrolysis for 10 min at 60°C, and Schiff's reagent for 2 h).

### Nuclear DNA Imaging Analysis

Excised vegetative (Fig. 1, S1) and prefloral (Fig. 1, S3) shoot apices were fixed in acetic acid:alcohol (1:3, v/v), rinsed with 70% (v/v) EtOH, rehydrated, and stained by the Feulgen reaction, as described above. We excised stained apical meristems under a microscope, then flattened and mounted them in DePex (Gurr, BDH, Poole, UK). An image-analysis system fitted with Ploidy 4.04 software (SAMBA 2005, Alcatel, TITN, Grenoble, France) performed nuclear DNA quantification. The mean 2C reference value ±2 SD was determined by analysis of half-telophases on both types of meristems and submitted to the Kolmogorov-Surinov test of normality. For each condition around 500, interphase nuclei were analyzed and ranged into histograms. We estimated the relative frequency of $G_0$-$G_1$ nuclei based on their position between the limits of the 2C distribution.

### Extraction, Purification, and Analysis of Cytokinins

We dissected the apices and froze them in liquid nitrogen, taking care to discard all young leaves. Twelve to fifteen apices were pooled, resulting in a sample of approximately 40 mg fresh weight. Samples were extracted overnight in Bieleski's solvent. Before centrifugation at 24,000*g* for 15 min at 4°C, we added deuterated standards for cytokinins (Apex International) and purified the extract using a combination of solid-phase and immunoaffinity purification, as described by Redig et al. (1996a). We performed a quantitative analysis of cytokinins using capillary column switching on a fully automated workstation (Famos, LC Packings, Amsterdam, The Netherlands) coupled to a liquid chromatography setup, consisting of an HPLC pump (model 325S, Kontron Instruments, Milan, Italy), an in-line UV detector (model 322, Kontron), and a triple-quadrupole MS (Quattro II, Micromass UK Ltd., Cheshire, UK).

Twenty-five-microliter sample aliquots were introduced into one dimension of the system using 10 mM $CH_3COONH_4$ as the mobile phase at a flow rate of 40 $\mu$L $min^{-1}$. Analytes were captured on a $C_{18}$ column (5 $\mu$m, 500 $\mu$m i.d. × 5 mm, LC Packings) for 7 min. A mobile phase switch for 5 min using 10 mM $CH_3COONH_4$ and water:methanol (30:70, v/v) at a flow rate of 7 $\mu$L $min^{-1}$ introduced the analytes onto the $C_{18}$ analytical column (5 $\mu$m, 300 $\mu$m i.d. × 150 mm; Adsorbosphere, Alltech, Laarne, Belgium). Diagnostic transition ions as described by Prinsen et al. (1995) recorded the cytokinin chromatograms in multiple-reaction-monitoring mode. Absolute detection limits ranged from 2 fmol for IP to 15 fmol for zeatin. Due to electrospray characteristics under the applied conditions, a lower sensitivity was obtained for zeatin and DHZ than for IP. A more detailed description of this technology will be presented elsewhere (E. Witters, K. Vanhoutte, W. Dewitte, I. Machackova, E. Benkova, W. Van Dongen, E. Esmans, and H.A. Van Onckelen, unpublished data). We calculated the results according to the principle of isotope dilution and expressed them in picomoles per gram fresh weight. Calculation of detection limits and errors took fresh weight and recovery into account.

### Preembedding Immunolocalization of Zeatin, IP, and DHZ

Shoot apices were fixed under a vacuum for 30 min in a 0.5% (v/v) glutaraldehyde and 3% (w/v) paraformaldehyde mixture in PBS (135 mM NaCl, 2.7 mM KCl, 1.5 mM $KH_2PO_4$, and 8 mM $K_2HPO_4$, pH 7.2). The samples were then stored in the fixative for 2.5 h at 4°C. Thick sections (30–50 $\mu$m) were cut with a vibratome (model 1000, Technical Products International, St. Louis, MO). When we used

enzyme-linked or colloidal gold-linked secondary antibodies for detection, we adapted 25% gelatin (w/v) in PBS as a support for cutting small samples such as apices. After mounting the samples in gelatin on a microscope slide, they were fixed for 30 min. Sections were collected in ice-cold PBS in the wells of a tissue-culture plate. The floating sections were transferred consecutively in blocking buffer (0.5% [w/v] BSA, and 0.1% [v/v] fish gelatin, 1% [v/v] normal sheep serum, 20 mM glycine, and PBS, 3 × 10 min) and in a 0.025% (v/v) Tween 20 solution in PBS for 10 min. Sections were incubated with primary antibody in diluted 1:100 blocking buffer, supplemented with 0.025% (v/v) of Tween 20 at 4°C overnight, followed by 1 h at room temperature.

After three 10-min washes with PBS, we administered the secondary antibody diluted in blocking buffer. Sheep anti-rabbit IgG (1/100, in blocking buffer) conjugated with either AP or FITC (Molecular Probes, Eugene, OR) was monitoried by either light microscopy (Axioscop, Zeiss) or confocal laser microscopy (MRC-600, Bio-Rad). Sections were incubated with secondary antibodies for 1 h at room temperature, followed by three 10-min washes with blocking buffer and two 10-min washes with PBS. Sections treated with AP conjugates were rinsed with Tris-HCl buffer (0.1 M and 2 mM $MgCl_2$, pH 9.6) and allowed to react in the presence of nitroblue tetrazolium and 5-bromo-4-chloro-3-indolyl phosphate (Bio-Rad) for 3 min. We added 2 mM EDTA in PBS to stop the enzymatic reaction. Samples were mounted in PBS:glycerin (50:50, v/v) containing 2 mM EDTA and observed immediately. After the rinsing steps (in darkness), we mounted the samples, treated with FITC-labeled goat anti-rabbit antibodies, in Mowiol (Harlow and Lane, 1988) to reduce fading during observation by confocal laser microscopy.

For preembedding ultrastructural immunolocalization, colloidal gold (<1 nm)-labeled secondary antibodies (1:40, Aurion, Wageningen, The Netherlands) were applied to the sections, revealing binding of the primary antibody. After five 10-min washes in PBS, a supplementary fixation with 1.6% (v/v) glutaraldehyde in PBS (15 min), followed by two 10-min rinses with deionized water (2 × 10 min), was performed prior to silver enhancement (SM kit, Amersham) of the colloidal gold (10 min). After washing with water, samples were dehydrated through an ethanol series and embedded in araldite (Fluka) via propylene oxide. Sections were embedded flat in the resin between the bottom of a silicon rubber embedding mold and a cover slip. After polymerization (48 h at 70°C), we selected areas of interest by light microscopy and placed a gelatin capsule filled with araldite upside down on the preparation, permitting polymerization. Coverslips were easily removed after cooling of the specimens with liquid nitrogen, and blocks were sectioned with a diamond knife on an ultramicrotome (LKB, Bromma, Sweden). Sections were collected on copper grids and stained with 6% uranyl acetate (w/v) and 0.3% (w/v) lead citrate in water for 10 min. We then observed the preparations with a transmission electron microscope (model 301S, Philips, Eindhoven, The Netherlands, or model 1200, Jeol) operated at 80 kV.

## RESULTS

### Growth Parameters and Meristematic Activity of Tobacco during Vegetative and Reproductive Development

The tobacco var Petit Havana cv SR1 is day neutral (the time of flowering is not affected by day length; McDaniel, 1992). To define the different sampling points, we determined some of the developmental characteristics of the vegetative and reproductive phases of the SR1 tobacco plants grown under our experimental conditions (Fig. 1). The shoot apical meristem entered a flowering stage after 5 to 6 weeks of vegetative growth, during which time 15 ± 1 leaves, nodes, and internodes were initiated. The switch to the prefloral transition phase was identified by the arrest of leaf initiation, accompanied by loss of the apical organization into lateral and central zones, and doming of the meristem (Fig. 5a). Inflorescence was initiated next, with the first floral meristems with sepals and petals observed on 7- to 8-week-old plants. Because the inflorescence in the *Nicotianaea* is a raceme of cymes, several stages of flower development were present on a single plant. Sampling during the reproductive phase concerned exclusively the terminal flowers.

During vegetative growth the mitotic activity in the apical meristems was highest in the lateral zones (mitotic

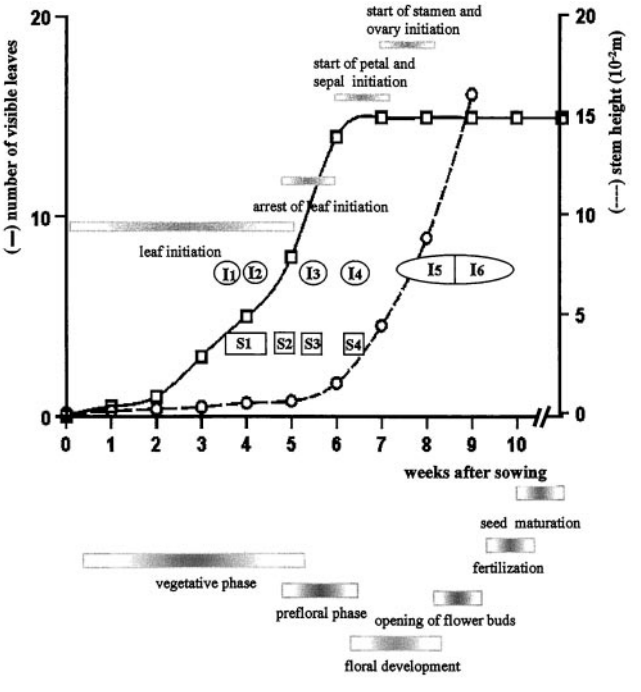


**Figure 1.** Summary of the main parameters of vegetative and reproductive development of the tobacco var Petit Havana cv SR1. The number of visible leaves and the stem height were recorded starting with an interval of 1 week, and were plotted against the number of weeks after sowing. Sampling points for both cytokinin quantification (S1–S4) and for immunolocalization of cytokinin bases (I1–I6) are located in the graph. The horizontal bars in the graph indicate the different morphogenetic events at the apical shoot meristem. The horizontal bars under the graph indicate the different phases of plant development.

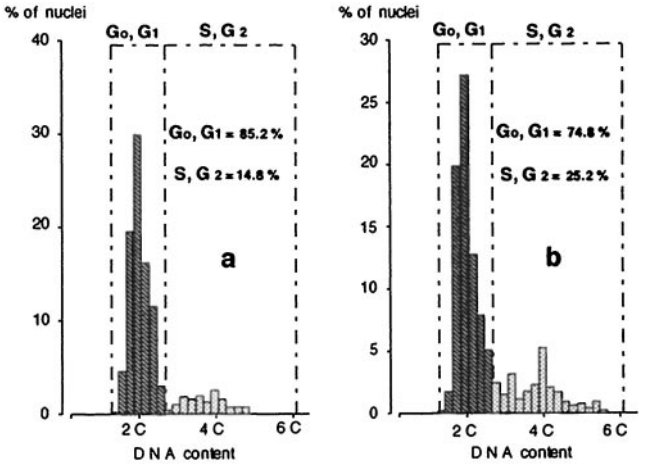


**Figure 2.** DNA content distribution in apices during the vegetative and prefloral transition phase. Histogram of the nDNA content during the vegetative phase (a) and the prefloral transition (b). The percentage of cells in $G_0$,$G_1$ and S,$G_2$ is also presented.

**Table II.** *Efficiency of the aldehyde mixture (3% [w/v] paraformaldehyde and 0.5% [v/v] glutaraldehyde in PBS) to link cytokinin bases (IP, DHZ, and zeatin) and cytokinin ribosides (IPA, DHZR, and ZR) to BSA and plant material*

| | BSA[a] | Plant Material[b] |
|---|---|---|
| | $A_{405}$ | % |
| BSA | 0.2 | – |
| IP | 3.1 | 23 |
| IPA | 0.5 | 6 |
| DHZ | 3.0 | 11 |
| DHZR | 0.2 | 2 |
| Zeatin | 3.0 | 11 |
| ZR | 0.2 | 2 |

[a] $A_{405}$ of the reaction product of the alkaline phosphatase. To reveal binding of cytokinin ribosides or bases to BSA, immunostaining with alkaline phosphatase linked to the secondary antibody was performed. [b] Percentage of radioactive tracer linked to 1 g of plant material. Coupling of radioactive cytokinin bases and ribosides to plant tissues was estimated by liquid scintillation, and the percentages were calculated toward the total amount of radioactivity used in the assay.

index = 6.9% ± 1.3), followed by the rib meristem (mitotic index = 4.9% ± 1.3), and the axial zone (mitotic index = 3.3% ± 0.3). In prefloral transition meristems, the mitotic activity in the axial zone increased (mitotic index = 4.9% ± 0.5), whereas the lateral zones (mitotic index = 7.1% ± 1.5) and the rib meristem (mitotic index = 6.4% ± 0.6) maintained their previous activity.

In addition, image analysis of DNA contents indicated that the nuclei of both vegetative and prefloral transition shoot apices were predominantly in $G_0$-$G_1$ (Fig. 2). The fraction of proliferating cells, revealed by the relative frequency of the S+$G_2$ nuclei, increased during the transition phase. Considering mitotic indices and DNA levels, we concluded that the prefloral condition is characterized by increased cell-cycling activity.

### Specificity of the Antibodies and Immobilization of Cytokinin Bases in Situ

Due to the ubiquity of adenine derivatives in living cells, the occurrence of cytokinins as modified nucleosides in the tRNA of some species (Vreman et al., 1974; Edwards and Armstrong, 1981; Sprinzl and Gauss, 1983), and the presence of isoprenylated proteins (Biermann et al., 1994), the immunolocalization of cytokinins requires highly specific antibodies. The three anti-cytokinin antibodies displayed significant cross-reactivity only with their respective free bases, ribosides, and 9-glucosides (Table I). The anti-ZR antibodies did not react with zeatin-*O*-glucoside. No cross-reactivity was found against yeast tRNA, *N*-acetyl-*S*-farnesyl-L-cystein, *N*-acetyl-*S*-geranyl-L-cystein, or *N*-acetyl-*S*-geranyl-geranyl-L-cystein, excluding possible artifacts

**Table I.** *Cross-reactivity of three different affinity-purified anti-cytokinin antibodies for different classes of cytokinins, yeast tRNA, and isoprenylated cysteins*

| | Anti-ZR | Anti-DHZR | Anti-IPA |
|---|---|---|---|
| | | % cross-reactivity[a] | |
| *trans*-ZR | 100 | 1 | <0.01 |
| *cis*-ZR | 4 | <0.3 | <0.3 |
| Zeatin | 60 | <0.3 | <0.01 |
| DHZR | <0.3 | 100 | <0.001 |
| DHZ | <0.3 | 16 | <0.3 |
| IPA | <0.3 | <0.01 | 100 |
| IP | <0.1 | <0.01 | 50 |
| DHZ-N9-glucoside | 1 | 80 | <0.1 |
| Zeatin-N9-glucoside | 68 | <0.3 | <0.1 |
| Zeatin-*O*-glucoside | <0.1 | <0.01 | <0.1 |
| Yeast tRNA | <0.01 | <0.01 | <0.01 |
| AFC, AGC, AGGC[b] | <0.01 | <0.01 | <0.01 |

[a] (pmol standard giving 50% displacement/pmol competitor giving the same displacement) × 100. [b] AFC, *N*-acetyl-*S*-farnesyl-L-cystein; AGC, *N*-acetyl-*S*-geranyl-L-cystein; AGGC, *N*-acetyl-*S*-geranylgeranyl-L-cystein.

caused by odd tRNA bases or by farnesylation, geranylation, or geranylgeranylation of proteins.

Immunostaining detected binding of cytokinin bases and ribosides by aldehyde fixation to BSA. The absorbance of the AP reaction product of wells in which the fixation solution included the cytokinin bases IP, DHZ, and zeatin was higher ($A_{405}$ = 3) than that measured in wells containing cytokinin ribosides or BSA ($A_{405}$ = 0.5) (Table II). Thus we can deduce that a short and weak aldehyde fixation resulted in the linkage of only cytokinin bases to BSA, and that the epitopes on the cytokinin bases were kept intact by this fixation.

We observed the same preferential binding of IP, DHZ, and zeatin in plant material upon aldehyde fixation of radioactive cytokinins (Table II). The slightly higher values observed for the isopentenyl-type cytokinins in the in planta test were probably caused by the more hydrophobic nature of these compounds. These results are in accordance with previous reports (Sossountsov et al., 1988). In contrast to *N*-glycosylated cytokinins that do not contain a reactive NH group, *O*-glucosides are retained by the fixative but are not recognized by the antibodies (Table I).

Bearing in mind that free bases and *O*-glucosides are preferentially linked in planta, and considering the absence of cross-reactivity of the anti-cytokinin antibodies for *O*-glucosides, we can conclude that the cytokinin bases zeatin, DHZ, and IP are selectively immunolabeled following the immunocytochemical process.

### In Situ Distribution of Cytokinin Bases in Vegetative and Reproductive Shoot Apices

During vegetative growth (Fig. 1, I1), the three cytokinin bases were present in apical shoot meristems and in leaf primordia (Fig. 3, a–c). At the end of the vegetative phase (Fig. 1, I2), we observed an overall decrease in immunolabeling. Whereas zeatin and IP were still detectable (Fig. 3, d and f), the signal of DHZ disappeared completely (Fig.

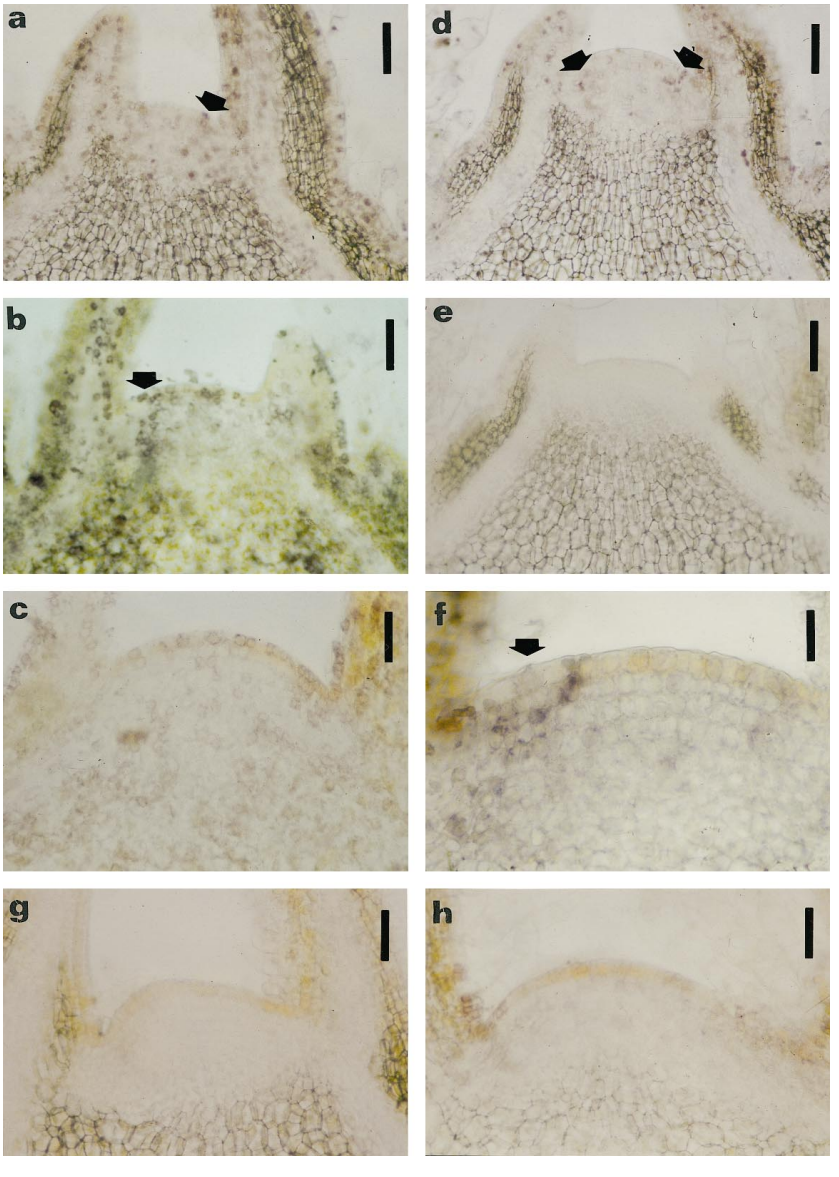


**Figure 3.** Immunolocalization of cytokinin bases within vegetative shoot apices. The location of cytokinin bases in longitudinal sections was determined using immunohistochemistry. Nitroblue tetrazolium/5-bromo-4-chloro-3-indolyl phosphate was used as chromogenic substrate for the AP, resulting in a purple reaction product. Immunolocalization of zeatin (a and d), DHZ (b and e), and IP (c and f) in vegetative shoot apices at developmental stages I1 (a, b, and c) and I2 (d, e, and f) (Fig. 1). Purple staining is present for zeatin (a and d) in the nucleus and cytoplasm, whereas for DHZ (b and e) and IP (c and f) a more perinuclear purple staining is visible. Arrows in a, b, d, and f point to staining in the lateral zones of the meristems. g and h, Sections (from stage I1, see Fig. 1) incubated with anti-zeatin (g) and anti-DHZ (h) antibodies saturated with zeatin and DHZ as a control, respectively. Bars = 90 $\mu$m (a, b, d, e, g, and h); 45 $\mu$m (c); and 22 $\mu$m (f).

3e). During the experiments it became apparent that some sections displayed a stronger immunolabeling in the lateral zone before the emergence of the leaf buttress (Fig. 3, a, b, d, and f), which could eventually be associated with the initiation of leaf primordia. When, as a control, we saturated the primary antibodies with their antigens, we observed a decrease in signal close to the limit of visual detection (Fig. 3, g and h). Omitting the primary antibody resulted in an absence of labeling (data not shown). Without counterstaining, all of the control sections displayed a yellow background conferred by phenolics in the first tunica layer of the meristem and in the various parenchyma. Cell outlines in differentiated tissues were visible due to light refraction at the level of the cell walls.

At higher magnification the compartmentation of the cytokinin bases DHZ and IP appeared mainly cytoplasmic and perinuclear. A very specific and pronounced nuclear labeling was observed on sections processed for zeatin localization (Figs. 3, a and d, and 4). We used ultra-small colloidal gold particles (Fig. 4, A and C) and a fluorescence probe (Fig. 4B) linked to the secondary antibody to check for artifacts caused by a nonspecific deposition of the AP reaction product. Both light microscopy and confocal laser microscopy revealed strong signals in the nuclei of some cells upon labeling for zeatin (Fig. 4, A and B). The nuclear appearance of this labeling was confirmed by electron microscopy. Silver particles resulting from the enhancement of colloidal gold particles were clearly present in the nucleus and cytoplasm of some cells (Fig. 4C).

The prefloral transition apex (Fig. 1, I3) was characterized by the total disappearance of detectable cytokinin bases in the apical meristem (Fig. 5a). Additionally, we observed a reduced immunostaining in the differentiated leaf and stem tissues and in the axillary buds (data not shown). The onset of flowering (Fig. 1, I4), which is marked by sepal and petal initiation, was accompanied by a progressive reappearance of the immunolabeling in the meristem and in the new perianth sections (Fig. 5, b and c), with zeatin being detectable (Fig. 5c) earlier than DHZ and IP (Fig. 5b). At the later stages of flower development (Fig. 1, I5 and I6), when carpels and stamens were formed, we observed a further increase in detectable cytokinin bases (Fig. 5d). Because all three anti-cytokinin antibodies gave similar results (except for the pronounced nuclear labeling of zeatin in some cells), only labeling of zeatin was presented for stages I5 and I6 (Figs. 5, d and e, and 6). The staining was particularly strong in sporogenous tissue and young pollen grains in developing anthers (Fig. 5e). Developing ovules (Fig. 6, a and b) were also labeled.

Among the ovular cells, the archesporial cell (Fig. 6b, arrow) and later the embryo sac were significantly labeled. At the end of stamen differentiation (Fig. 1, I6), no label was found in mature pollen grains, whereas the vascular bundle of the connective and the cells of the longitudinal slits provided with secondary thickenings were highly labeled (data not shown). The vascular strands of the placenta were heavily stained as well (data not shown). After

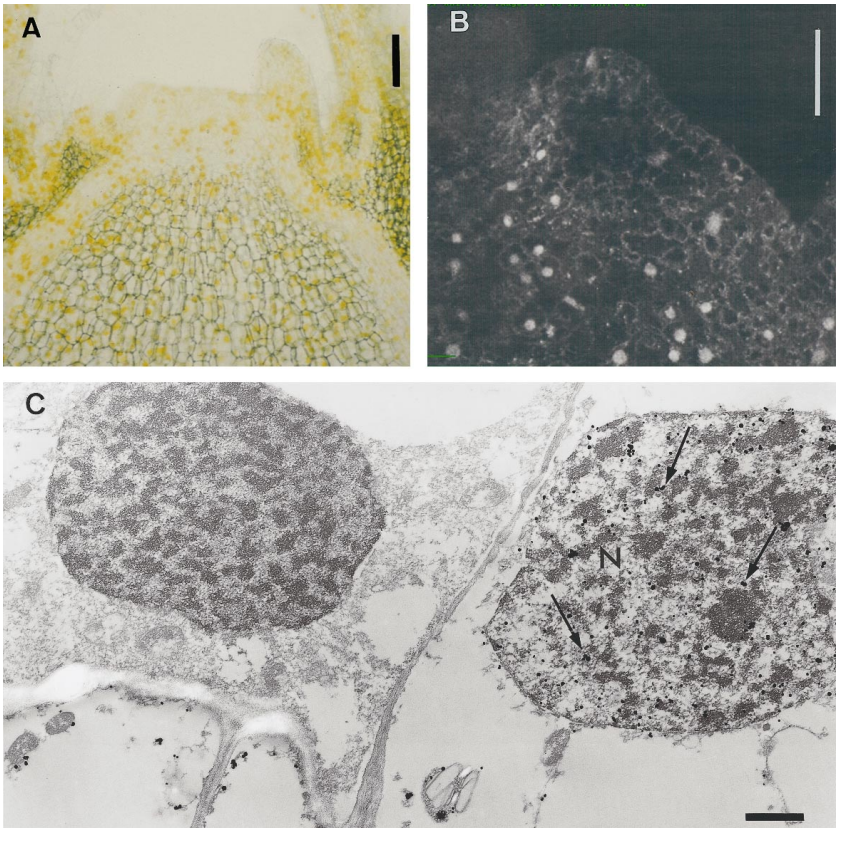


**Figure 4.** Immunolocalization of zeatin in vegetative shoot apices. Zeatin was localized in the nucleus of vegetative meristem cells upon silver-enhanced gold-labeling by light and electron microscopy (A and C). A, Yellow color, originating from light diffraction by the silver particles, was distributed throughout the apex. C, A large number of silver particles (arrows) were detected in the nucleus (N) of some cells by electron microscopy. Confocal laser microscopy after immunolocalization with FITC as a probe revealed a strong fluorescence signal in the nucleus of some cells (B). Bars = 90 $\mu$m (A), 100 $\mu$m (B), and 1 $\mu$m (C).

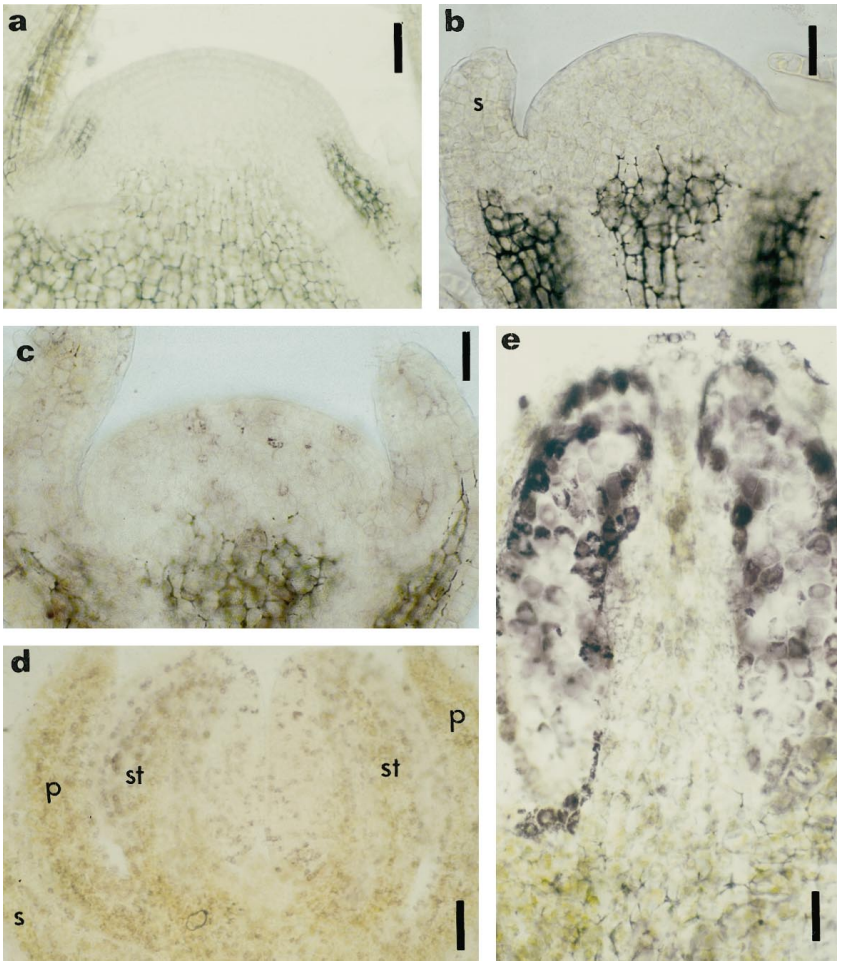


**Figure 5.** Immunolocalization of zeatin and IP in prefloral and floral shoot apices. Longitudinal sections of a prefloral transition apex (a), early floral apices (b and c), and floral apices (d and e) subjected to immunohistochemistry for zeatin (a, c, d, and e) and IP (b). Localization was with AP-conjugated secondary antibodies and nitroblue tetrazolium/5-bromo-4-chloro-3-indolyl phosphate as the chromogenic substrate. a, Prefloral transition apex immunostained for zeatin, disclosing no reaction of the AP in the meristem. b and c, Early floral phase with sepal formation showing the absence of label for IP (b), but the presence of reaction with the anti-zeatin antibody was reflected in weak purple staining (c). d and e, Floral phase with sepal, petal, and stamen already initiated; a strong purple staining occurred in different cells throughout the developing flower after immunostaining of zeatin. e, Longitudinal section of a developing stamen immunolabeled with anti-zeatin, showing a strong signal in the sporogenic tissue. p, Petal; s, sepal; st, stamen. Bars = 90 $\mu$m (a) and 45 $\mu$m (b, c, d, and e).

fertilization we observed strong cytoplasmic labeling both in the endosperm and in the embryo (Fig. 6c).

These observations during the development of tobacco shoot apices were highly reproducible; we obtained similar results for three different populations of plants arising from sowing at different dates.

### Quantification of Endogenous Cytokinins in the Shoot Apex

By means of capillary column switch technology, in combination with tandem MS, endogenous cytokinins could be measured with high sensitivity in minute plant samples. This methodology permitted quantification of 11 cytokinins in a single pool of 12 to 15 apices, representing approximately 40 mg fresh weight. Results of these analyses are presented in Table III. No *N*-glucoside cytokinin conjugates were detected in any of the samples analyzed (detection limit, 0.5 pmol $g^{-1}$ fresh weight). About 10 pmol $g^{-1}$ fresh weight of cytokinin bases were recorded in samples S1 (Fig. 1), corresponding to vegetative apices still initiating leaves, nodes, and internodes. No cytokinin bases could be detected during the lapse between the arrest of leaf formation and the initiation of flower buds (Fig. 1, S2 and S3). Cytokinin ribosides were present in all samples analyzed, and a correlation with the kinetics of the free bases was observed. Indeed, significantly lower riboside concentrations coincided with nondetectable levels of cytokinin bases in samples S2 and S3 (Fig. 1). Compared with ZR and IPA, consistently lower concentrations of DHZR were found. Initiation of flower parts (Fig. 1, S4) coincided with increased levels of both free bases and ribosides.

## DISCUSSION

By using aldehyde fixation (Sossountsov et al., 1988) in combination with affinity-purified antibodies for immunocytochemical analysis of nonembedded sections, we obtained new and accurate information on the distribution of the cytokinin bases zeatin, DHZ, and IP. The absence of embedding medium resulted in a high antigenicity and a low background. No artifactual tRNA labeling was observed, which was confirmed experimentally by the absence of signal in the prefloral transition stage. Although some reports indicate the presence of cytokinins as modified bases next to the anticodon in tobacco (Murai et al., 1975), the sterical organization of the tRNA probably obstructed recognition by the antibodies. This preembedding technology coupled with the use of specific antibodies proved to be very accurate for a highly specific localization

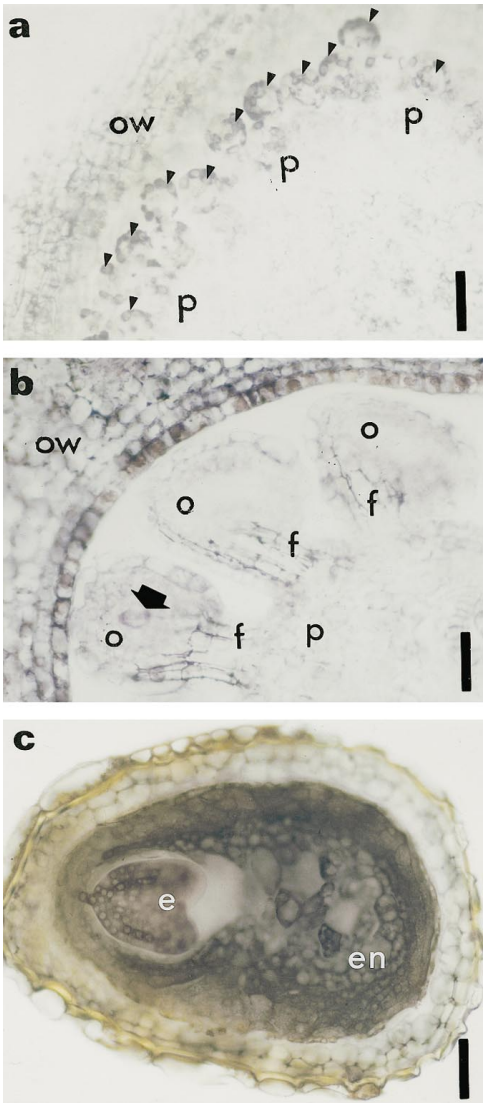


**Figure 6.** Immunolocalization of zeatin at two stages of ovule formation and at the end of seed formation. Cross-sections of ovule primordia arising from the placenta (a, arrowheads) and developing ovule (b, arrow indicates the archesporial cell in a developing ovule). Purple staining resulting from labeling of zeatin was detected in ovule primordia (a, arrowheads), the ovary wall (a and b), and the developing ovules (b). Archesporial cells are also significantly labeled (b). c, Cross-section of a seed immunolabeled with anti-zeatin antibody. The cytoplasm of embryo and endosperm are heavily stained. e, Embryo; en, endosperm; f, funiculus; o, ovule; ow, ovary wall; p, placenta. Bars = 180 $\mu$m (a) and 90 $\mu$m (b and c).

of the three cytokinin bases. A good correlation was also obtained between quantification of cytokinin bases by HPLC-tandem MS and results obtained by immunolocalization. The absence of immunostaining in the prefloral transition meristem coincided with an endogenous cytokinin base content below the detection limit. In flowering buds, cytokinin bases became detectable by both techniques. Data on the endogenous cytokinin content in dissected apices ($\pm$1.5 mm$^3$) could only be obtained with a capillary HPLC column switch system linked to an electrospray-tandem MS.

The presence of detectable free cytokinin bases, as measured by both immunocytochemistry and tandem MS, was positively correlated with increased concentrations of the cytokinin ribosides. This suggests that threshold amounts of ribosides could be required to produce detectable amounts (>1–2 pmol g$^{-1}$ fresh weight) of free cytokinin bases by the action of adenosine nucleosidases (Letham and Palni, 1983).

Our results show, for the first time to our knowledge, that immunocytochemistry can provide reliable qualitative and quantitative information on the cellular distribution of specific cytokinins.

Using these techniques we studied the kinetics of the endogenous levels and cellular localization of specific cytokinins in shoot apices developing from vegetative to reproductive functioning. In extracts of vegetative apices that initiate leaves, we detected nodes and internodes, significant amounts of zeatin, DHZ, IP bases, and ribosides by HPLC-tandem MS. The concentrations found for the free bases (varying around 10 pmol g$^{-1}$ fresh weight) were apparently sufficient to produce a clear signal in most of the cells when the anti-IPA antibody was used. We observed a more patchy signal when using both the anti-ZR and anti-DHZR antibodies. Because the overall concentration of the three bases was quite similar, this observation might be a reflection of a less homogenous distribution of zeatin and DHZ. Toward the end of the vegetative phase, the signal observed for all three cytokinin bases decreased significantly, reflecting the transition of the vegetative apex toward a prefloral status.

This prefloral phase, during which the shape of the meristem changed from flat to dome, was characterized by the arrest of leaf initiation and the loss of the apical organization into lateral and central zones. In contrast to what was described for white mustard (Gonthier et al., 1987), the nuclear DNA quantification in tobacco prefloral apices disclosed no blocking of cells in $G_2$. Moreover, an overall mitotic activity of about 6% indicated that during the prefloral phase meristematic cell division proceeded normally, with an increase in the $S+G_2$ fraction of the nuclei population. The absence of organogenesis during this phase coincided with significantly decreased endogenous cytokinin levels in the meristem. The riboside concentrations dropped to less than 50% of the values observed in vegetative meristems, whereas the concentration of free bases dropped even below detection limits.

These quantitative HPLC-tandem MS data matched exactly the immunocytochemical observations, with no labeling used for any of the anti-cytokinin antibodies. Once cytokinin concentrations increased again, as detected both by HPLC-tandem MS and immunolabeling, organogenesis resumed, with the initiation of petals and sepals. During further development of the flowers, all vascular strands and developing reproductive tissues were strongly labeled. This observation might be indicative for a sink effect of areas with high division activity, both mitotic and meiotic.

Previously reported results on increased cytokinin levels during flower development (Bernier et al., 1988; Lejeune et al., 1988, 1994; de Bouillé et al., 1989) in other species pointed to a putative role for cytokinins in floral evocation.

**Table III.** *Endogenous cytokinin bases and riboside concentration in apical shoot meristems at different developmental stages ±SE (S1–S4 as described in Fig. 1)*

| Developmental Stages and Features[a] | Zeatin | DHZ | IP | ZR | DHZR | IPA |
|---|---|---|---|---|---|---|
| | | | *pmol $g^{-1}$ fresh wt* | | | |
| S1<br>10 Leaves<br>5 to 6 Weeks | 8.7 ± 0.9 | 11.7 ± 1.2 | 12.4 ± 1.3 | 48.9 ± 4.8 | 9.4 ± 0.9 | 39.6 ± 3.9 |
| S2<br>13 Leaves<br>5 to 6 Weeks | ≤2.0 | ≤2.0 | ≤0.4 | 15.8 ± 1.5 | 3.9 ± 0.4 | 13.1 ± 1.3 |
| S3<br>15 Leaves<br>6 to 7 Weeks | ≤3.0 | ≤3.0 | ≤0.4 | 21.3 ± 2.1 | 5.9 ± 0.6 | 17.4 ± 1.7 |
| S4<br>15 Leaves<br>7 to 8 Weeks | 16.7 ± 1.7 | 13.1 ± 1.3 | 15.2 ± 1.6 | 97.4 ± 9.7 | 26.2 ± 2.6 | 43.5 ± 4.3 |

[a] See Figure 1.

However, the decreasing cytokinin levels in tobacco apical meristems at the end of the vegetative phase and the complete disappearance of free cytokinin bases during the reorganization of the meristem prior to flowering (being reported here for the first time to our knowledge), may incite a re-evaluation of the question as to whether cytokinins positively regulate the switch from a vegetative toward a floral meristem.

Earlier work in *Chenopodium* showed that after the photoperiodic induction of flowering, cytokinin content decreased (Machackova et al., 1993). Exogenous cytokinin application after the inductive photoperiod also inhibited flowering in this species (I. Machackova, personal communication). Recently, by measuring the cytokinin content in xylem sap, Beveridge et al. (1996, 1997) demonstrated that root-derived cytokinins do not control flowering in pea. Apparently, changes in the levels of endogenous cytokinins in the shoot apex itself (not just in leaves or other parts of the plant) seem to be involved in the flowering transition.

Although it is certainly premature to propose a general conceptual framework for the role of cytokinins in flowering, the results presented in this report may introduce some new insights on the involvement of cytokinins in the functioning of the apical meristem of tobacco plants. It can be concluded from our results that relatively high endogenous cytokinin levels are correlated with organogenesis (either vegetative or reproductive). Estruch et al. (1991, 1993) showed that upon expression of the *Agrobacterium tumefaciens ipt* gene, the enhanced endogenous cytokinin content resulted in adventitious vegetative buds on leaves of vegetative plants and flower buds on leaves of flowering plants. Our observations support the idea that enhanced cytokinin levels are essential for cell differentiation and organogenesis, but not for floral evocation in the strictest sense. This seems to be substantiated by the observation that during the prefloral phase, when floral evocation apparently occurs, no organogenesis takes place, a phenomenon that eventually may prove to be provoked by the significantly reduced cytokinin levels.

Another interesting observation involved the preembedding immunolocalization technique. In both vegetative and floral apices, we found a patchy nuclear labeling, but only when using anti-zeatin antibodies. These results indicate that among the free bases only zeatin is detectable in nuclei. Both confocal laser microscopy and electron microscopy confirmed the presence of zeatin in some nuclei, as was observed by using AP-conjugated secondary antibodies. This is the first report, to our knowledge, of such differential behavior of the different cytokinin types, which might be related to a specific function of the zeatin cytokinin types at the nuclear level in tobacco.

This nuclear labeling observed with anti-zeatin antibody is intriguing in light of the observations made by Redig et al. (1996b). By using a synchronized cytokinin autotrophic cell culture (BY2) (Nagata et al., 1992), they found that only zeatin was present during the whole-cell cycle, with a short, transient accumulation of this cytokinin type at the end of the S phase and during the M phase. One might be tempted to correlate the patchy appearance of the nuclear label with these specific phases in the cell cycle. However, the absence of label from prefloral apices, in which mitosis proceeds throughout the meristem at the same rate as in the lateral zones of vegetative apices, seems to contradict this assumption. It is possible that this is a matter of concentration and detection limits. Nevertheless, the nuclear compartmentation observed exclusively for the zeatin-type cytokinins provides good experimental evidence that, at least in tobacco, a specific mode of action within the nucleus might be attributed to zeatin. Colocalization experiments on zeatin with nuclear-marker proteins (Hemerly et al., 1992) for specific phases of the cell cycle are planned.

The practical approach for immunolocalization of cytokinins described in this paper opens new perspectives to address the cellular and molecular functions of cytokinins in plant growth and development. It has already permitted the introduction of some novel aspects of the involvement of cytokinins in the transition from a vegetative to a reproductive apex. We were also able to show the possibility of a unique mode of action at the nuclear level for cytokinins of the zeatin type. Because a good correlation was found between immunostaining and endogenous cytokinin lev-

els, as measured by HPLC-tandem MS, this immunocytochemical technique will prove to be helpful in identifying cytokinin-driven events, such as the regulation of gene expression at the cell and tissue levels.

## ACKNOWLEDGMENTS

The authors wish to thank Dr. M.S. Tsuji for advice on preembedding methodology, Dr. D. Stickens and Dr. T. Weiha for operation of the confocal microscope, W. van Dongen for help on tandem mass spectrometry, and I. Bernaert and M. Prouteau for skillful sectioning. Dr. W. Jacob and Dr. J.P. Verbelen are gratefully acknowledged for the use of the electron and confocal microscopes. The authors are also thankful to Dr. P.B. Gahan and Dr. D. Inzé for critical reading of the manuscript.

Received July 6, 1998; accepted September 9, 1998.

## LITERATURE CITED

**Bernier G** (1988) The control of floral evocation and morphogenesis. Annu Rev Plant Physiol Plant Mol Biol **39:** 175–219

**Besnard-Wibaut C** (1981) Effectiveness of gibberellins and 6-benzyladenine of flowering of *Arabidopsis thaliana*. Physiol Plant **53:** 205–212

**Beveridge CA, Murfet IC, Kerhoas L, Sotta B, Miginiac E, Rameau C** (1997) The shoot controls zeatin riboside export from pea roots: evidence from the branching mutant *rms4*. Plant J **11:** 339–345

**Beveridge CA, Ross JJ, Murfet IC** (1996) Branching in pea. Action of genes *Rms3* and *Rms4*. Plant Physiol **110:** 859–865

**Biermann BJ, Morehead AT, Tate ST, Price JF, Randhall SK, Crowell DN** (1994) Novel isoprenylated proteins identified by an expression library screen. J Biol Chem **269:** 25251–25254

**de Bouillé P, Sotta B, Miginiac E, Merrien A** (1989) Hormones and inflorescence development in oilseed rape. Plant Physiol Biochem **27:** 443–450

**Deikman J, Ulrich M** (1995) A novel cytokinin-resistant mutant of *Arabidopsis* with abbreviated shoot development. Planta **195:** 440–449

**Eberle J, Wang TL, Cook S, Wells B, Weiler EW** (1987) Immunoassay and ultrastructural localization of isopentenyladenine and related cytokinins using monoclonal antibodies. Planta **172**: 289–297

**Edwards CA, Armstrong DJ** (1981) Cytokinin-active ribonucleosides in *Phaseolus* RNA. Distribution in tRNA species from etiolated *P. vulgaris* L. seedlings. Plant Physiol **67:** 1185–1189

**Erlanger BF, Beiser SM** (1964) Antibodies specific for ribonucleosides and ribonucleotides and their reaction with DNA. Biochemistry **52:** 68–74

**Estruch JJ, Granell A, Hansen G, Prinsen E, Redig P, Van Onckelen H, Schwarz-Sommer Z, Sommer H, Spena A** (1993) Floral development and expression of floral homeotic genes are influenced by cytokinins. Plant J **4:** 379–384

**Estruch JJ, Prinsen E, Van Onckelen H, Schell J, Spena A** (1991) Viviparous leaves produced by somatic activation of an inactive cytokinin-synthesizing gene. Science **254:** 1364–1367

**Gonthier R, Jacqmard A, Bernier G** (1987) Changes in cell-cycle duration and growth fraction in the shoot meristem of *Sinapis* during floral transition. Planta **170:** 55–59

**Harlow E, Lane D** (1988) Cell staining. *In* E Harlow, D Lane, eds, Antibodies, a Laboratory Manual. Cold Spring Harbor Laboratory Press, Cold Spring Harbor, NY, p 418

**Hemerly A, Bergounioux C, Van Montagu M, Inzé D, Ferreira P** (1992) Genes regulating the plant cell cycle: isolation of a mitotic-like cyclin from *Arabidopsis thaliana*. Proc Natl Acad Sci USA **89:** 3295–3299

**Ivanova MI, Todorov IT, Atanassova L, Dewitte W, Van Onckelen HA** (1994) Co-localization of cytokinins with proteins related to cell proliferation in developing somatic embryos of *Dactylis glomerata* L. J Exp Bot **45:** 1009–1017

**Laloue M, Pethe C** (1982) Dynamics of cytokinin metabolism in tobacco cells. *In* PF Wareing, ed, Plant Growth Substances, 1982. Academic Publishers, New York, pp 185–195

**Lejeune P, Bernier G, Requier MC, Kinet J** (1994) Cytokinins in phloem and xylem saps of *Sinapis alba* during floral induction. Physiol Plant **90:** 522–528

**Lejeune P, Kinet JM, Bernier G** (1988) Cytokinin fluxes during floral induction in the long day plant *Sinapis alba* L. Plant Physiol **86:** 1095–1098

**Letham DS, Palni LMS** (1983) The biosynthesis and metabolism of cytokinins. Annu Rev Plant Physiol **34:** 163–197

**Machackova I, Krekule J, Eder J, Seidlova F, Strnad M** (1993) Cytokinins in photoperiodic induction of flowering in *Chenopodium* species. Physiol Plant **87:** 160–166

**Mok MC** (1994) Cytokinins and plant development: an overview. *In* DWS Mok, MC Mok, eds, Cytokinins: Chemistry, Activity and Function. CRC Press, Boca Raton, FL, pp 155–166

**Murai N, Armstrong DJ, Skoog F** (1975) Incorporation of mevalonic acid into ribosylzeatin in tobacco callus ribonucleic acid preparations. Plant Physiol **55:** 853–858

**Nagata T, Nemoto Y, Hasezawa S** (1992) Tobacco BY-2 cell line as the "HeLa" cell in the cell biology of higher plants. Int Rev Cytol **132:** 1–30

**Prinsen E, Redig P, Van Dongen W, Esmans E, Van Onckelen HA** (1995) Quantitative analysis of cytokinins by electrospray tandem mass spectrometry. Rapid Commun Mass Spectrom **9:** 948–953

**Redig P, Schmülling T, Van Onckelen H** (1996a) Analysis of cytokinin metabolism in *ipt* transgenic tobacco by liquid chromatography-tandem mass spectrometry. Plant Physiol **112:** 141–148

**Redig P, Shaul O, Inzé D, Van Montagu M, Van Onckelen H** (1996b) Levels of endogenous cytokinins, indole-3-acetic acid and abscisic acid during the cell cycle of synchronised BY-2 cells. FEBS Lett **391:** 175–180

**Skoog F, Miller CO** (1957) Chemical regulation of growth and organ formation in plant tissues cultured *in vitro*. Symp Soc Exp Biol **11:** 118–131

**Sossountzov L, Maldiney R, Sotta B, Sabbagh I, Habricot Y, Bonnet M, Miginiac E** (1988) Immunocytochemical localization of cytokinins in *Craigella* tomato and a sideshootless mutant. Planta **175:** 291–304

**Sotta B, Stroobants C, Sossountsov L, Maldiney R, Miginiac E** (1990) Immunocytochemistry applied to cytokinins: techniques and their validation. *In* M Kaminek, DWS Mok, E Zazimalova, eds, Physiology and Biochemistry of Cytokinins in Plants. SPB Academic Publishing, The Hague, The Netherlands, pp 455–460

**Sprinzl M, Gauss DH** (1983) Compilation of transfer RNA sequences and modified nucleosides in transfer RNA. *In* PF Agris, RA Kopper, eds, The Modified Nucleosides of Transfer RNA. II. Alan R. Liss, New York, pp 129–226

**Strnad M, Peters W, Beck E, Kaminek M** (1992) Immunodetection and identification of $N^6$-(*o*-hydroxybenzylamino)purine as a naturally occurring cytokinin in *Populus* × *canadensis* Moench leaves. Plant Physiol **99:** 74–80

**Venglat SP, Shawney VK** (1996) Benzylaminopurine induces phenocopies of floral meristem and organ identity mutants in wild-type *Arabidopsis* plants. Planta **198:** 480–487

**Veselý J, Havlicek L, Strnad M, Blow J, Donella-Deana A, Pinna L, Letham DS, Kato JY, Detivaud L, Leclerc S, and others** (1994) Inhibition of cyclin-dependent kinases by purine analogues. Eur J Biochem **224:** 771–786

**Vreman HJ, Schmitz RY, Skoog F, Playtis AJ, Frihart CR, Leonard NJ** (1974) Synthesis of 2-methylthio-*cis*- and *trans*-ribosylzeatin and their isolation from *Pisum* tRNA. Phytochemistry **13:** 31–37

**Zavala ME, Brandon DL** (1983) Localization of a phytohormone using immunocytochemistry. J Cell Biol **97:** 1235–1239

**Zhang K, Letham DS, John PCL** (1996) Cytokinin controls the cell cycle at mitosis by stimulating the tyrosine dephosphorylation and activation of $p34^{cdc2}$-like H1 histone kinase. Planta **200:** 2–12